



Kinetic analysis of the inhibition of the drug efflux protein AcrB using surface plasmon resonance



Rumana Mowla^a, Yinhu Wang^b, Shutao Ma^b, Henrietta Venter^{a,*}

^a School of Pharmacy and Medical Sciences, Sansom Institute for Health Research, University of South Australia, SA 5000, Australia

^b Department of Medicinal Chemistry, Key Laboratory of Chemical Biology, School of Pharmaceutical Sciences, Shandong University, Jinan 250012, China

ARTICLE INFO

Keywords:

Multidrug resistance
Drug efflux
Efflux pump inhibitor
Affinity constant
Surface plasmon resonance
AcrB

ABSTRACT

Multidrug efflux protein complexes such as AcrAB-TolC from *Escherichia coli* are paramount in multidrug resistance in Gram-negative bacteria and are also implicated in other processes such as virulence and biofilm formation. Hence efflux pump inhibition, as a means to reverse antimicrobial resistance in clinically relevant pathogens, has gained increased momentum over the past two decades. Significant advances in the structural and functional analysis of AcrB have informed the selection of efflux pump inhibitors (EPIs). However, an accurate method to determine the kinetics of efflux pump inhibition was lacking. In this study we standardised and optimised surface plasmon resonance (SPR) to probe the binding kinetics of substrates and inhibitors to AcrB. The SPR method was also combined with a fluorescence drug binding method by which affinity of two fluorescent AcrB substrates were determined using the same conditions and controls as for SPR. Comparison of the results from the fluorescent assay to those of the SPR assay showed excellent correlation and provided validation for the methods and conditions used for SPR. The kinetic parameters of substrate (doxorubicin, novobiocin and minocycline) binding to AcrB were subsequently determined. Lastly, the kinetics of inhibition of AcrB were probed for two established inhibitors (phenylalanine arginyl β -naphthylamide and 1-1-naphthylmethyl-piperazine) and three novel EPIs: 4-isobutoxy-2-naphthamide (A2), 4-isopentyloxy-2-naphthamide (A3) and 4-benzyloxy-2-naphthamide (A9) have also been probed. The kinetic data obtained could be correlated with inhibitor efficacy and mechanism of action. This study is the first step in the quantitative analysis of the kinetics of inhibition of the clinically important RND-class of multidrug efflux pumps and will allow the design of improved and more potent inhibitors of drug efflux pumps. This article is part of a Special Issue entitled: Beyond the Structure-Function Horizon of Membrane Proteins edited by Ute Hellmich, Rupak Doshi and Benjamin McIlwain.

1. Introduction

Antibiotic resistance is a global problem that needs urgent attention [53,63,71]. The World Health Organisation has recently listed 12 families of bacteria that pose the greatest threat to human health. All the organisms listed as “priority-1” (critical level) are Gram-negative bacteria [72]. Gram-negative bacteria display high levels of intrinsic resistance due to the presence of an outer membrane that act as a permeability barrier and the expression of an array of drug efflux pumps [3,5,21,24] which lowers the concentration of antibiotics inside the cell to sub-toxic levels. Clinical levels of resistance in Gram-negative bacteria are conferred by transporters that consist of complex, macromolecular, tripartite assemblies that span the double membrane and periplasm of these organisms such as the AcrAB-TolC efflux system from *Escherichia coli* [2,5,9,10,12,21,30,35–38,57]. In these complexes an inner membrane protein (e.g. AcrB) acts together with an outer

membrane protein (e.g. TolC) and a periplasmic adaptor protein (e.g. AcrA) to form a highly efficient antibiotic efflux system [11,14,16,45,65,67]. The inner membrane protein is from the resistance nodulation division (RND) and is the component responsible for drug recognition and binding [17,25,32,33,39,54]. Therefore, compounds which can directly block the drug binding to AcrB by binding with higher affinity or allosterically trap the IMP in an inactive conformation, are attractive forms of efflux pump inhibitors (EPIs) [13,42,44,64].

The first structures of AcrB in an asymmetric homotrimeric conformation [25,47] not only provided the first structural information on these intractable membrane proteins, but also allowed the deduction of a possible transport mechanism. These structures revealed a functional rotation mechanism where the three monomers cycle through three different conformations during the efflux process designated the loose/access, tight/binding and open/extrusion stages [25,47]. In the ensuing

* Corresponding author.

E-mail address: rietie.venter@unisa.edu.au (H. Venter).

years significant advances have been made in the structural and functional determination of AcrB [15,17,31,39,74]. The binding site of AcrB was revealed to be large with two major substrate-binding pockets located along the substrate translocation pathway. The access binding pocket is located closer to the periplasmic bulk in the access/loose monomer of the transport cycle. The deep binding pocket is located much deeper within the substrate transport pathway, and is wide open in the binding/tight monomer of the transport cycle [42–44]. The two binding pockets are separated by a flexible glycine-rich loop. Conformational flexibility of this loop (termed the switch loop) is crucial to allow the conformational changes that drive antibiotic efflux [8,18,28].

These structural and biochemical data was followed by the first structures of inhibitor-bound AcrB which constitutes a significant advance in the field. The structure of the pyranopyrimidine inhibitor D13-9001 bound to AcrB [29] and MX2319 bound to AcrBper (periplasmic domain of AcrB) [50] suggested tight binding of these inhibitors to the narrow hydrophobic pit lined by several phenylalanine residues which prevents the functional rotation of AcrB necessary for drug extrusion and prevent the efflux of antibiotics [29]. EPs such as phenylalanine arginyl β -naphthylamide (PA β N) and 1-(1-naphthylmethyl)-piperazine (NMP) are shown to straddle the top of the switch loop in molecular dynamics simulation studies [59]. This interaction with the switch loop, in turn, controls the movement of substrates in the deep binding pocket and was the proposed mechanism of action of these two EPs [42]. PA β N and NMP act at concentrations of $\geq 50 \mu\text{M}$ [6,23]. A derivative of MX2319, MBX3132 binds AcrB with nanomolar affinity as a result of a tight interaction between this compound and residues from the hydrophobic trap [50]. Cryo-electron microscopy of the full tripartite complex confirmed that this inhibitor prevents the functional rotation and traps AcrB predominantly in the symmetric tight/binding conformation [67]. The idea that a (too) high affinity of compounds for the deep binding pocket could prevent the conformational changes necessary for RND-transporters to cycle through the functional rotation was first suggested by Vargiu et al. [58] to interpret MIC changes due to mutations within this pocket. Structural studies are invaluable in our understanding of the interaction of inhibitors with efflux proteins. However, an inhibitor-bound structure provides a snapshot of the process only at one specific time. Computational techniques are a great resource to address mechanistic knowledge gaps, as they can pinpoint functional dynamics of biological systems and has been used to great effect to compare binding of a range of substrates and inhibitors to AcrB. However, MD simulation studies need to be complemented with experimental data.

Nakashima et al. [29] measured the binding affinity of D13-9001 to purified AcrB, MexB, and MexY using isothermal titration calorimetry (ITC). K_d values of 1.15 μM and 3.5 μM respectively for AcrB and MexB were obtained. The biggest limitation of ITC is the large amount of purified protein needed for each substrate that is analysed, which makes this method impracticable for the routine analysis of membrane proteins. Progress on the measurement of kinetic constants was further hampered by the huge contribution of non-specific binding of the lipophilic drugs to these hydrophobic proteins to the total binding observed. The voluminous binding cavity and redundancy in active site residues also meant it is not possible to provide a binding-negative mutant of these proteins to correct for non-specific binding. We included the galactose permease protein GalP, an integral sugar binding protein of similar hydrophobicity to AcrB [62] as control for non-specific drug binding. The kinetics of substrate and inhibitor binding to AcrB were subsequently probed using surface plasmon resonance (SPR). SPR is a very powerful biophysical tool for drug discovery which allows real time monitoring of binding events as well as directly measure affinity and kinetic constants of biomolecular interactions [41]. The major advantage of SPR over other techniques is it does not require particular labelling (e.g. fluorescence or radioactive) to analyse molecules. Moreover, the amount of ligand required is much less than is required in other techniques (such as ITC) which are particularly

beneficial for membrane-proteins such as AcrB [41,56]. The method is also scalable to high throughput format.

2. Methods

2.1. Plasmids used

Expression plasmid coding for AcrB with 8-His tags at C-terminal (pAcrB) and expression plasmid coding for GalP with 6-His tags at C-terminal (pGalP) both containing kanamycin resistant marker were used for expression of respective proteins [40,70]. Kanamycin was used at 25 $\mu\text{g}/\text{mL}$.

2.2. Preparation of inside out vesicles (ISO) vesicles

Cells were always freshly transformed with plasmid before use. A single transformant was inoculated and grown overnight at 37 °C in LB broth containing kanamycin. To ensure high level expression, the cultures were incubated at 18 °C until an OD₆₆₀ of around 0.2 before gene transcription was induced with 0.5 mM isopropyl β -D-1-thiogalactopyranoside (IPTG). Growth was continued with shaking at 200 rpm overnight to allow expression of the target protein [48]. The cells were harvested by centrifugation (15 min, 6500g, 4 °C) and resuspended in 0.1 M potassium phosphate (pH 7.0). DNase (10 $\mu\text{g}/\text{mL}$) and MgSO₄ (10 mM) were added and the suspension was incubated for 15 min at RT before being passed twice through a cell disruptor (Constant Systems with Thermoflex Temperature control) at 20 kPsi. The suspension was incubated at room temperature for 15 min to allow the DNase to act. A low speed centrifugation (10 min, 10,000g, 4 °C) was performed to remove cell debris (pellet), and the supernatant was subjected to high-speed centrifugation using a 50.2 Ti rotor (40,000g, 40 min, 4 °C) to collect the inside out vesicles (ISO vesicles). The pellet was re-suspended in 50 mM potassium phosphate buffer pH 7.0 containing 10% glycerol to a protein concentration of approximately 50 mg/mL and stored at –80 °C. The protein concentration of the inside-out membrane vesicles was determined by the D_C Protein Assay (Bio-Rad Laboratories) with BSA (0 to 1.5 mg/mL) as a standard.

2.3. Purification of his-tagged proteins

GalP protein was overexpressed in *E. coli* C41 (DE3) cells and purified by affinity chromatography according to established protocols [62,68]. Purification of AcrB was essentially the same as previously reported for MexB [48] with some modifications as indicated. The ISO vesicles prepared from cells expressing required proteins were allowed to solubilise (20 mM Tris pH 8.0, 10% glycerol, 300 mM NaCl, 1.5% DDM and 10 mM imidazole pH 8.0) for an hour at room temperature through gentle shaking. Unsolubilised protein was removed by ultracentrifugation (150,000 $\times g$, 1 h, 4 °C). Ni-NTA (Ni²⁺-nitrilotriacetate) resin (Bio-Rad) was equilibrated by washing with 20 resin volumes of deionized water, gravity sedimentation on ice and resuspended with 5 resin volumes of wash buffer A (20 mM Tris pH 8.0, 10% glycerol, 300 mM NaCl, 0.05% DDM and 30 mM imidazole pH 8.0). The supernatant from the ultracentrifugation was added to the Ni-NTA resin and the protein was allowed to bind to the resin by gentle shaking for 1 h at 4 °C. The resin was transferred to a 2 mL polystyrene mini-column (BioRad laboratories) and the unbound fraction was allowed to drain away. The resin in the column was washed with 30 resin volumes of wash buffer A and subsequently with 30 resin volumes of wash buffer B (20 mM K-HEPES pH 7.5, 10% glycerol, 300 mM NaCl, 0.05% DDM and 50 mM imidazole pH 8.0). Five resin volumes of elution buffer (20 mM K-HEPES pH 7.5, 10% glycerol, 300 mM NaCl, 0.5% DDM and 400 mM imidazole pH 8.0) were added to displace the His-tagged protein from the resin. The first 0.5 resin volume of eluant was discarded. The next 3–4 resin volumes of eluant were collected as the purified His-tagged protein. Total purified protein was determined using a microvolume spectrophotometer (Denovix).

2.4. Fluorescent drug binding assay

The basis of this assay is the large increase in fluorescence of the substrates when in a non-aqueous environment such as within the membrane or bound to protein as opposed to their being practically non-fluorescent in an aqueous environment. Binding of fluorescent substrates Hoechst 33342 or 1-(4-trimethylammoniumphenyl)-6-phenyl-1,3,5-hexatriene p-toluenesulfonate (TMA-DPH) to purified protein was carried out in 2 mL reaction mixtures containing 25 µg of purified protein in 10 mM Bis-Tris pH 7.2. Hoechst 33342 or TMA-DPH was added to the solution in a stepwise fashion to a final concentration of 4 µM when no major changes in fluorescence were detected anymore. Measurements were performed in an LS-55B luminescence spectrometer (Perkin Elmer). The excitation and emission wavelengths for the dyes were 355 nm and 457 nm respectively for Hoechst 33342 and 350 nm and 425 nm respectively for TMA-DPH. The excitation and emission slits were 10 nm and 4 nm respectively for Hoechst 33342 and 5 nm and 4 nm respectively for TMA-DPH. As a control and to correct for non-specific binding, binding assays was carried out in a similar manner with an equimolar amount of GalP, a 12-helix membrane sugar transport protein of similar hydrophobicity as AcrB [62].

2.5. Measuring kinetic constants with surface plasmon resonance (SPR)

A Biacore T200 biosensor system (GE Healthcare) was used to characterise binding interactions. The surface of a CM-5 chip was activated with a 1:1 mixture of N-hydroxysuccinimide and 1-ethyl-3-(3-dimethylamino) propyl carbodiimide which converts carboxylates on the dextran matrix into succinamide esters. These are highly reactive with primary amines (lysine residues and the N-terminus of proteins and peptides). Purified AcrB (0.5 mg/mL) was first desalted and then diluted 10 times in immobilisation buffer (10 mM Na-acetate pH 4.5). AcrB was then immobilised on the activated surface chip by amine coupling in 1.05 x PBS + 0.05% Tween 20 by injecting it over flow cell 2 for 2100 s. After AcrB immobilisation, the untreated succinamide groups was quenched with 50 mM Tris pH 7.4. Purified GalP was similarly treated and injected over flow cell 4 until the same RU was reached as for AcrB (typically around 20,000 RU). The control cells (flow cell 1 and 3) received the same treatment except they were treated with only immobilisation buffer instead of the proteins.

A number of the compounds studied in this project were only soluble in DMSO. To study kinetic behavior of these analytes, running buffer B (running buffer A containing 5% DMSO) was used to flow continuously over the flow cells whereas the sample solutions for analysis was prepared in such a way that the DMSO concentration was maintained at 5%. In this way, a large signal difference created by the difference in refractive indexes of solvents could be avoided. However, there is always the risk of DMSO concentration being varied slightly between different samples. The effect of these variations is usually small in terms of absolute response, but still significant in kinetic studies where minor differences in response units could potentially contribute to wrong interpretation of data. To avoid this, the solvent correction wizard designed in Biacore T200 by GE healthcare was utilised. Solvent correction is applied during the runs and adjusts difference in bulk response. The solvent correction stock solutions with 4.5% and 5.8% DMSO were prepared following instructions from GE Healthcare Life Sciences in 'Buffer and sample preparation for direct binding assay in 5% DMSO'. Serial dilutions of inhibitors and substrates were prepared in running buffer B in such a way that the DMSO concentration was 5%. Standard 96-well plates were used for analytes, where 8 compounds could be studied at 11 different concentrations. The first well for all the compounds contained only running buffer B and represents zero analyte. The run started with five start up cycles to stabilise the baseline. The solvent correction solutions were injected over control and active surfaces and was repeated after 30 and 60 cycles of analyte injection. Analytes were injected through all the flow cells, under continuous

flow. The association and dissociation times were set at 60 s and 120 s respectively. DMSO (50%) was used for washing. As the analyte binds to the ligand, the change/increase in refractive index caused by the interaction was viewed as response units (RU) versus time (a sensogram).

2.6. Curve fitting and statistical analyses

The difference in RU (Δ RU) between binding to AcrB and GalP was plotted against the substrate/inhibitor concentration. The binding constants B_{\max} and K_d were determined using the relationship $B_{\max}[S] / (K_d + [S])$, in which drug binding is represented by B, the drug concentration by [S], the maximal binding by B_{\max} , and the drug concentration yielding $1/2B_{\max}$ by the dissociation constant K_d . All analysis was performed in Prism.

3. Results

3.1. Preparation of ISOVs and purification of proteins

The sugar transport protein GalP was used as a control for non-specific binding since GalP is also a hydrophobic protein containing 12 TMH just like AcrB and similar to AcrB also assemble in homotrimers [75]. However, GalP is selective for sugars [62]. AcrB and GalP were purified from ISO membrane vesicles prepared from the *E. coli* C41 (DE3) expression strain harbouring the pAcrB and pGalP protein expressing plasmids respectively. Protein production was induced at 18 °C for optimal protein expression [48]. Under these conditions AcrB and GalP constituted roughly 25% of the total membrane proteins in the ISO vesicles (Fig. 1). The proteins were purified by Ni-NTA resin affinity chromatography by exploiting the C-terminal His tags. Both proteins could be purified to high homogeneity with typical yields of around 1–2 mg pure protein per litre of culture (Fig. 1).

The discrepancy between the exact Mw of proteins and the Mw observed in SDS-PAGE, as seen for GalP (Fig. 1B), is not uncommon for integral membrane proteins. These proteins often run anomalously on SDS-PAGE due to differential detergent binding and improper unfolding [49,69].

3.2. Determination of kinetics of substrate binding to AcrB using fluorescence

The binding affinity of Hoechst 33342 and TMA-DPH for AcrB was determined by a drug-binding assay that utilise the unique fluorescent properties of these dyes. These dyes are non-fluorescent in aqueous solution, whereas when bound to the hydrophobic binding pocket of a protein, an increase in fluorescence quantum yield is observed. Equimolar amounts of AcrB and GalP were titrated with increasing concentrations of dyes. The fluorescence was measured after each addition to yield the total amount of binding. Specific binding was obtained by subtracting the fluorescence values obtained for GalP (non-specific binding) from that of AcrB (total binding). The results (specific binding) were plotted against the concentrations of the substrates. The data were fitted with a one binding site hyperbola and yielded binding constants (K_d) of $1.14 \pm 0.09 \mu\text{M}$ and $0.57 \pm 0.04 \mu\text{M}$ for Hoechst 33342 and TMA-DPH respectively (Fig. 2).

Although this fluorescence measurement is a convenient and well-established way to determine binding of ligands to membrane proteins [4,61,70,73] its use is limited to fluorescent substrates that undergo a significant change in fluorescence upon binding to the protein. Therefore, we sought to adapt this technique for use in a label-free technique such as SPR.

3.3. Binding affinity of Hoechst 33342 and TMA-DPH determined by SPR

To determine the suitability of SPR for binding of these hydrophobic

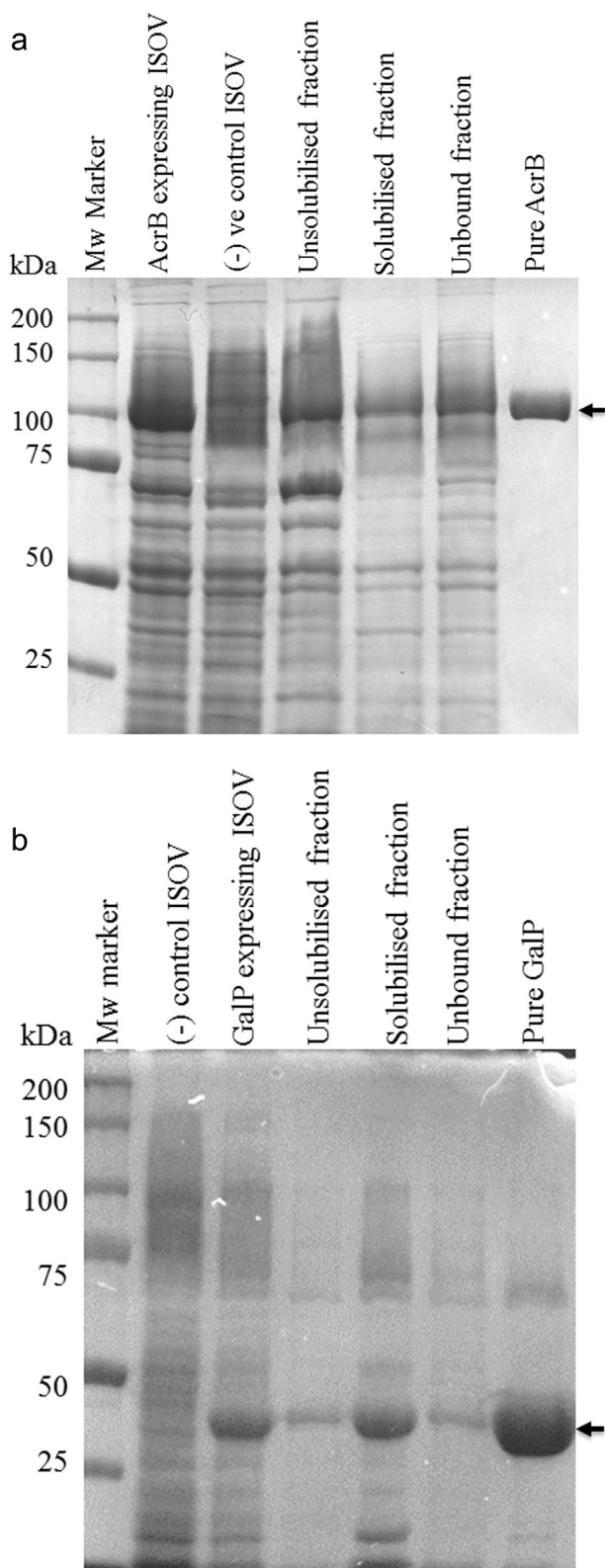


Fig. 1. AcrB can be purified to high homogeneity. ISO vesicles made from cells that propagated pAcrB (A) or pGalP (B) were used as positive control and ISO vesicles prepared from cells harbouring the pET41 non-expressing control plasmid was used as negative control. Samples were collected from each stage of protein purification and separated on a 10% SDS-PAGE gel. Proteins were visualised with Coomassie Brilliant Blue. Purified AcrB (MW = 112 kDa) and GalP (MW = 51 kDa) are indicated by arrows in A and B respectively. (For interpretation of the references to colour in this figure legend, the reader is referred to the web version of this article.)

substrates to integral membrane proteins, the binding constants of Hoechst 33342 and TMA-DPH to AcrB were determined in the first instance and compared to the K_d values obtained with fluorescence. Purified AcrB and GalP were covalently immobilised to the dextran matrix of a CM5 chip by amine coupling to yield RU values of $\sim 22,000$. A series of concentrations for each dye was injected and the change in signal (Δ RU) for each concentration was noted. Binding of the dyes to both proteins occurred very fast therefore the kinetic parameters could only be obtained by plotting the Δ RU against the concentration of dye (Fig. 3). For Hoechst, (concentration 0.03125–12.5 μ M) binding affinity was in the range of 1.25 to 2.05 μ M. A representative data set is presented in Fig. 3. The K_d value obtained with SPR correlates very well with the $1.15 \pm 0.07 \mu$ M obtained with the fluorescent binding method. The K_d obtained for TMA-DPH (concentration range 0.03125–12.5 μ M) was $0.76 \pm 0.23 \mu$ M, which also was in a range obtained from fluorescent drug binding (Table 1).

3.4. Determination of the kinetics for AcrB-substrate interactions

Subsequently, the binding affinities of substrates novobiocin, minocycline and doxorubicin were determined. All these substrates displayed dissociation constants in the μ M range. K_d values of $7.5 \pm 2.0 \mu$ M and $9.9 \pm 3.0 \mu$ M were obtained for doxorubicin and novobiocin respectively. Minocycline seemed to bind most strongly with the protein and the affinity constants were always in the range of 1 to 1.8 μ M. Representative data are presented in Fig. 4.

3.5. Determination of the kinetics for AcrB-inhibitor interactions with SPR

The ultimate aim was to dissect the kinetics of efflux pump inhibition to aid the design of EPIs, therefore the binding constants of the inhibitors PA β N and NMP to AcrB were determined. We also determined the kinetic parameters of AcrB inhibition of three novel 2-naphthamide compounds selected from a series of fourteen compounds. Among the three, A3 had proven EPI activity synergising with three AcrB substrates. The two other inhibitors selected for this study were A2 and A9 which synergised with erythromycin and chloramphenicol respectively in a resistant phenotype of *E. coli* [65,67]. PA β N displayed a surprisingly low affinity for AcrB with K_d values ranging from 15 to 28 μ M. A representative curve is presented in Fig. 5A. On the other hand, the inhibitor NMP bound to AcrB with much higher affinity than PA β N with a K_d of 0.488 ± 0.1 , (Fig. 5B). Among the three novel compounds A2, A3 and A9, the dissociation constants for A2 and A3 were $1.5 \pm 0.3 \mu$ M and $2.99 \pm 0.84 \mu$ M respectively. Binding of A9 to AcrB was weaker than for A2 and A3 ($K_d = 24.57 \pm 8.2 \mu$ M). The results are and shown in Fig. 5 and listed in Table 1.

4. Discussion

The development of compounds that inhibit drug efflux and thereby synergise with antibiotics to reverse antimicrobial resistance is of major importance in the fight against antimicrobial resistance [34,42,44,51,52,64,66]. An understanding of the kinetics of inhibition would be of great importance in the design and synthesis of the efflux pump inhibitors. Although great strides have been made in the structural basis of AcrB inhibition [29,50] and the kinetics of drug efflux [19,20,27], the kinetics of inhibition is still to a great extent uncharted territory. We addressed the lack of knowledge by establishing a reliable SPR method for the kinetic analysis of the interactions of substrates and inhibitors with AcrB. Measuring specific binding of small lipophilic molecules to large, hydrophobic drug efflux proteins has been hampered by the many non-specific hydrophobic sites in these proteins. The binding site of AcrB contains multiple binding possibilities with different functionalities even more so than that of AcrD, another RND-type drug efflux pump from *E. coli* [43]. As a result of the voluminous binding cavity and redundancy in active sites, it is not possible to

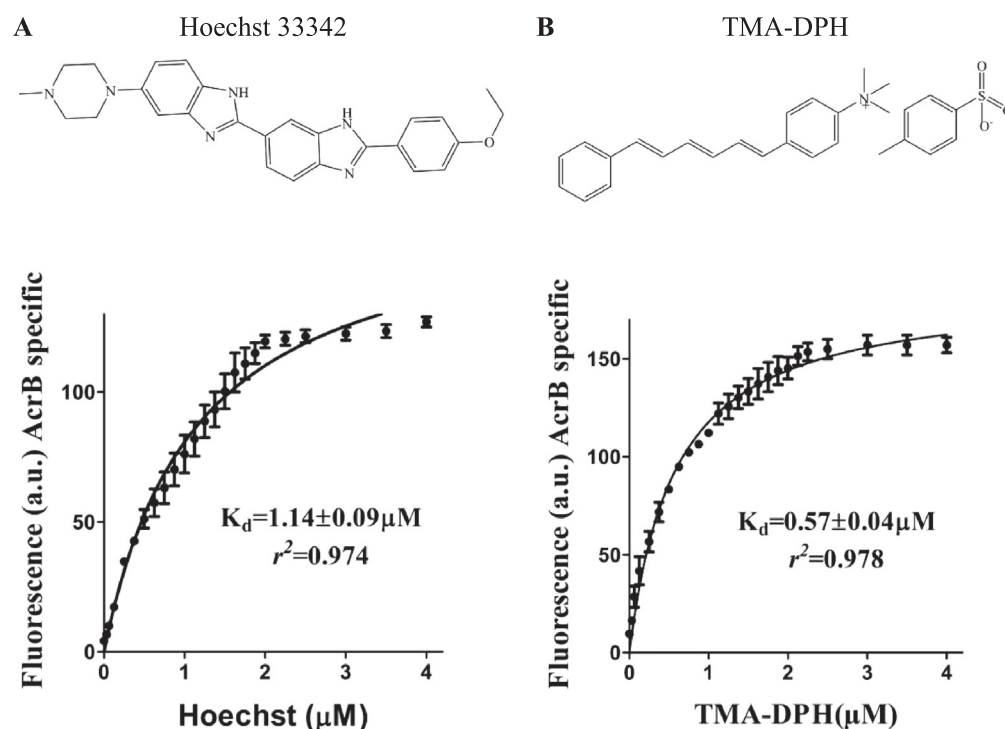


Fig. 2. Chemical structures and kinetics of binding of two fluorescent substrates to purified AcrB using a fluorescence assay. Upper Panel: Chemical structure of (A) Hoechst 33342 and (B) TMA-DPH. Lower panel: Kinetics of substrate binding to AcrB using fluorescence. Binding of (A) Hoechst 33342 and (B) TMA-DPH to purified AcrB was measured by fluorimetry in the presence of increasing concentrations of the dyes. The data were corrected for non-specific binding and fitted to a one-site specific binding hyperbola. Results are means \pm S.E.M. of three independent experiments with protein purified from different batches of vesicles.

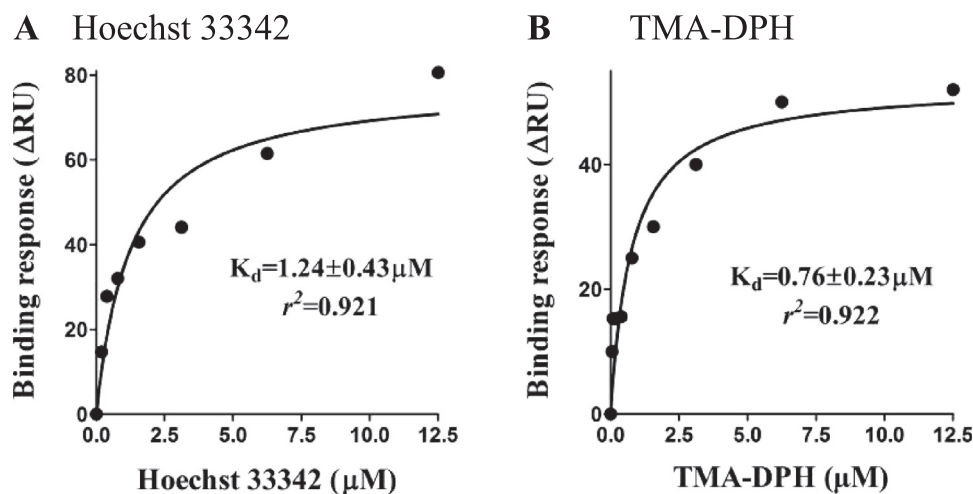


Fig. 3. Kinetics of binding of two fluorescent substrates to purified AcrB using SPR. The signals obtained for the specific binding of (A) Hoechst 33342 and TMA-DPH to AcrB were plotted against the concentrations of the dyes used. Data were analysed by fitting into a one-site specific binding hyperbola to obtain K_d . Results are representative of three independent experiments repeated on different days with different batches of purified protein.

Table 1
The equilibrium dissociation constants of substrates and inhibitors for AcrB as determined by fluorescence and SPR.

		Equilibrium dissociation constant K_d (μM)	
		Fluorometric method	SPR
Substrates	Hoechst 33342	1.14 ± 0.09	1.3 ± 0.5
	TMA-DPH	0.58 ± 0.04	0.77 ± 0.23
	Doxorubicin	–	7.5 ± 2.0
	Minocycline	–	1.88 ± 0.56
Inhibitors	Novobiocin	–	9.90 ± 3.0
	PA β N	–	15.72 ± 3.0
	NMP	–	0.5 ± 0.1
	A2	–	1.5 ± 0.3
	A3	–	2.99 ± 0.84
	A9	–	24.6 ± 8.2

construct a binding negative mutant to these proteins. Mutants of AcrB in which the phenylalanine residues in the binding site were changed individually or in combination, displayed only a minor reduction in the ability to confer resistance and only to some of the tested substrates [7]. In order to correct non-specific binding, we have developed an SPR technique that uses a sugar transport protein of similar hydrophobicity to AcrB in order to probe the binding kinetics of substrates and inhibitors to the drug efflux protein AcrB. A combination of *in silico* screening and SPR have also been employed with great success to identify inhibitors of the soluble AcrA component of the AcrAB-TolC efflux pump [1]. The ability to screen and characterise inhibitors against the integral membrane protein AcrB reported here is therefore a significant advance in the field.

To confirm the validity of the method designed for SPR, we first determined dissociation constants for two fluorescent substrates of AcrB, namely Hoechst 33342 and TMA-DPH using a well-established

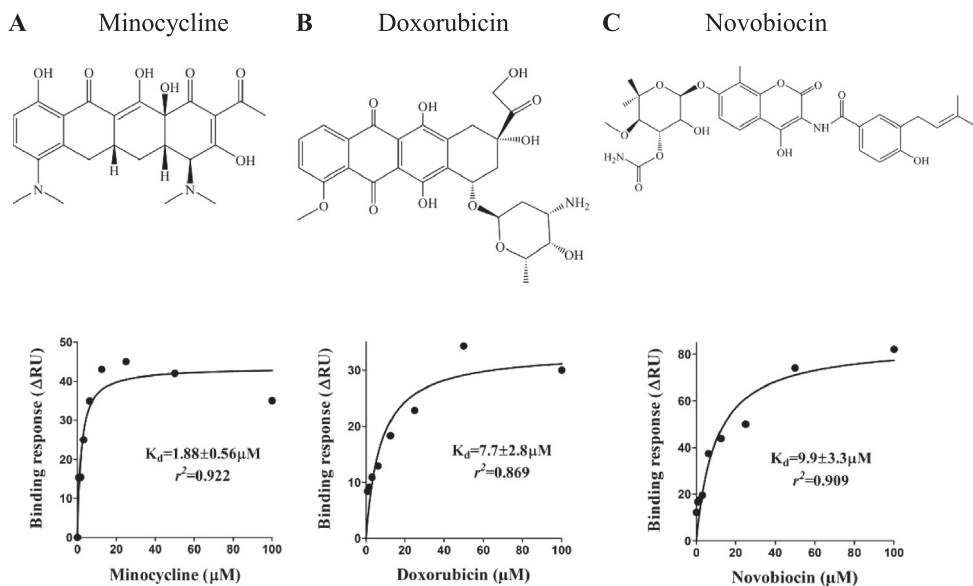


Fig. 4. Chemical structures and kinetic parameters of binding of substrates to purified AcrB using SPR. Upper Panel: Chemical structures of (A) minocycline, (B) doxorubicin and (C) novobiocin. Lower panels: ΔRU for substrate-AcrB interactions were plotted against the concentrations of the substrates used. Data were analysed by fitting into a one-site specific binding hyperbola to obtain K_d . Results are representative of three independent experiments repeated on different days with different batches of purified protein.

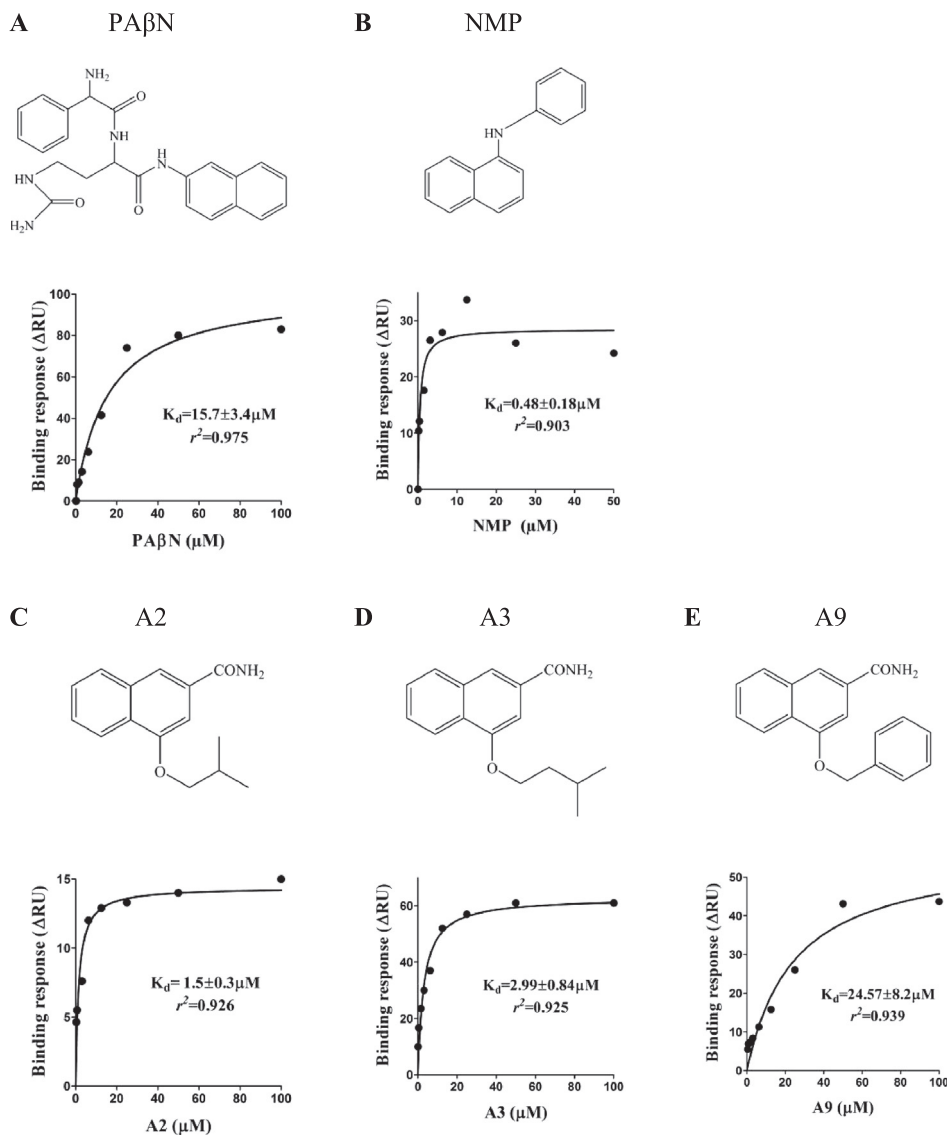


Fig. 5. Chemical structures and kinetic parameters of binding of inhibitors to purified AcrB using SPR. Upper Panel: Chemical structures of (A) PAβN, (B) NMP, (C) A2, (D) A3 and (E) A9. Lower panels: ΔRU for inhibitor-AcrB interactions were plotted against the concentrations of the inhibitors used. Data were analysed by fitting into a one-site specific binding hyperbola to obtain K_d . Results are representative of three independent experiments repeated on different days with different batches of purified protein.

fluorometric binding assay [4,61,70,73]. We observed a very good correlation between the kinetic constants obtained with the two different methods. Among the substrates tested, relatively weaker binding affinity was found for doxorubicin ($K_d = 7.5 \pm 2.0 \mu\text{M}$) than for minocycline ($K_d = 1.88 \pm 0.5 \mu\text{M}$). The crystal structure of AcrB bound with minocycline and doxorubicin showed differences in the amino acid residues they interact with which might contribute to their different binding affinities. Minocycline interacted with Gln 176 and Phe 178 whereas doxorubicin interacted with Asn 274 and Phe 178 [18]. The binding affinity of novobiocin was found to be similar to doxorubicin ($K_d = 9.9 \pm 3.0 \mu\text{M}$). There are no crystal structures of AcrB bound to novobiocin available. However, the data obtained for these three substrates supported a previous finding from docking simulations studies where the free energy of binding predicted for novobiocin and doxorubicin were similar (-9.2 kcal). In contrast to our results though, minocycline was predicted to bind with a lower affinity than doxorubicin and novobiocin (free energy of binding predicted to be -8 kcal) [54]. Another study reported a K_d for novobiocin binding to AcrB of 6 mM [55]. This value is implausibly large as the concentration range tested was only between 25 and 200 μM and is more likely to be a reflection of the absence of correction for non-specific binding.

The SPR method was further employed to interrogate the action of two established inhibitory compounds (PA β N and NMP) and three novel EPs (A2, A3 and A9; [65,67]). PA β N is very effective in the reversal of resistance [23], however it appears to bind AcrB with a relatively low affinity compared to the substrates minocycline, doxorubicin and novobiocin. The modest affinity of PA β N to the pump agrees with previous findings showing that this compound is rapidly pumped out by AcrB and with K_M values one order of magnitude larger than that of a strong substrate such as nitrocefin [19,20]. One possible explanation for this discrepancy between the efficacy of PA β N as an inhibitor of efflux and its low affinity for AcrB could be the well-known outer membrane permeabilising effect of PA β N which is responsible for its synergistic activity rather than competition with the substrate [22]. High-throughput screening for EPs should therefore not only include methods such as SPR, but also cell based assays to capture compounds that synergise with antibiotics through outer membrane permeabilisation [46]. On the other hand, NMP bound with a much higher affinity ($K_d = 0.48 \pm 0.1 \mu\text{M}$) than PA β N and also has a higher affinity for AcrB than the substrates tested (even though NMP and PA β N act as inhibitors at the same concentrations). This affinity is slightly higher, but in the same range as that of the inhibitor D13-9001 where a K_d value of 1.15 μM was obtained for the binding of this inhibitor to AcrB [29]. Although NMP and D13-9001 display comparable binding affinities to AcrB, NMP is an efficient inhibitor of efflux in *E. coli*, while the reversal of resistance of D13-900 seems to be only effective in *P. aeruginosa* [26]. This most likely indicate that the activity of D13-900 are reliant on its outer membrane permeabilisation through a selective outer membrane channel in *P. aeruginosa*.

The results obtained for the three-novel compounds provided further confirmation of the in silico and biological data on the identification of EPs. A3, the best EPI candidate synergised with three substrates (erythromycin, chloramphenicol and tetraphenyl phosphonium). The equilibrium dissociation constant of $2.99 \pm 0.84 \mu\text{M}$ which was significantly lower than that of PA β N but larger than that of NMP. It is worth noting that unlike PA β N, A3 did not have any non-specific effect on the bacterial cells. Compound A9 synergised with one substrate (chloramphenicol) only and the K_d obtained for A9 was $24 \pm 8 \mu\text{M}$; indicating weaker binding of the compound with AcrB than A3 and explained why it did not synergise with more AcrB substrates. Moreover, in the Nile red efflux assay, the efflux-inhibitory activity of A9 was only achieved at the fairly high concentration of 500 μM as compared to 100 μM required for A3 [65,67],

indicating that A9 acted as competing substrate instead of an inhibitor. A9 also displayed some outer membrane permeabilising effect which could account for its ability to reduce resistance to antibiotics. Compound A2, which only synergised with erythromycin, had a similar binding affinity ($K_d = 1.5 \pm 0.3 \mu\text{M}$) to A3. The affinity of these 2-naphthamide derivatives (A2 and A3) seemed to be related to the extension of the C-4 side chains (Fig. 5) in the hydrophobic cavity. It is known that F136, F178, F610, F615 and F628 are contributing to the free energy of binding of all the MBX compounds [50,60]. A2, with the shortest side chain, shows similar affinity than A3 with the longer side chain while A9, with a benzene ring at the same position, display a ten times lower affinity. As A2 and A3 has comparable affinities, and only a one carbon difference in the side chain, the reason why A2 does not synergise with as many substrates as A3 is not entirely clear.

In this study, we have standardised and optimised a method for determining the kinetics of substrate and inhibitor binding to AcrB. We have succeeded to correct for non-specific binding of substrates and inhibitors to AcrB by using GalP; an integral membrane protein of comparable hydrophobicity, but which recognise only galactose. We demonstrated that SPR could be used as a highly sensitive, label-free tool to accurately measure the affinity constants for ligands binding to purified AcrB. The kinetic data obtained could also be correlated with inhibitor efficacy and mechanism of action. To our knowledge, this is the first time that specific binding to an RND transporter could be measured and accurate binding constants could be derived. This SPR method would provide the means for studying the interactions of other drug transporters with their substrates and inhibitors. Moreover, there is no need for labelling of either protein or substrate and hence no limit on the compounds that could be studied and this method is also scalable for high throughput analysis of kinetics.

Acknowledgements

The authors thank Paolo Ruggerone and Attilio V Vargiu (University of Cagliari) for critical reading of the manuscript and helpful discussions. This research was supported financially by the China-Australia Centre for Health Sciences Research grant (2014GJ06 and 2016GJ, HV and SM) and Australian Postgraduate Award (RM).

References

- [1] N. Abdali, J.M. Parks, K.M. Haynes, J.L. Chaney, A.T. Green, D. Wolloscheck, J.K. Walker, V.V. Rybenkov, J. Baudry, J.C. Smith, H.I. Zgurskaya, Reviving antibiotics: efflux pump inhibitors that interact with AcrA, a membrane fusion protein of the AcrAB-TolC multidrug efflux pump, *ACS Infect Dis* 3 (2017) 89–98.
- [2] S. Alibert, J. N'gompaza Diarra, J. Hernandez, A. Stutzmann, M. Fouad, G. Boyer, J.M. Pages, Multidrug efflux pumps and their role in antibiotic and antiseptic resistance: a pharmacodynamic perspective, *Expert Opin. Drug Metab. Toxicol.* 13 (2017) 301–309.
- [3] M. Arzanlou, W.C. Chai, H. Venter, Intrinsic, adaptive and acquired antimicrobial resistance in gram-negative bacteria, *Essays Biochem.* 61 (2017) 49–59.
- [4] A. Bapna, L. Federici, H. Venter, S. Velamakanni, B. Luisi, T.P. Fan, H.W. Van Veen, Two proton translocation pathways in a secondary active multidrug transporter, *J. Mol. Microbiol. Biotechnol.* 12 (1) (2007) 97–209.
- [5] J.M. Blair, G.E. Richmond, L.J. Piddock, Multidrug efflux pumps in gram-negative bacteria and their role in antibiotic resistance, *Future Microbiol* 9 (2014) 1165–1177.
- [6] J.A. Bohnert, W.V. Kern, Selected arylpiperazines are capable of reversing multidrug resistance in *Escherichia coli* overexpressing RND efflux pumps, *Antimicrob. Agents Chemother.* 49 (2005) 849–852.
- [7] J.A. Bohnert, S. Schuster, M.A. Seeger, E. Fahnrich, K.M. Pos, W.V. Kern, Site-directed mutagenesis reveals putative substrate binding residues in the *Escherichia coli* RND efflux pump AcrB, *J. Bacteriol.* 190 (2008) 8225–8229.
- [8] H.J. Cha, R.T. Muller, K.M. Pos, Switch-loop flexibility affects transport of large drugs by the promiscuous AcrB multidrug efflux transporter, *Antimicrob. Agents Chemother.* 58 (2014) 4767–4772.
- [9] M. Chitsaz, M.H. Brown, The role played by drug efflux pumps in bacterial multidrug resistance, *Essays Biochem.* 61 (2017) 127–139.
- [10] S. Coyne, P. Courvalin, B. Perichon, Efflux-mediated antibiotic resistance in *Acinetobacter* spp, *Antimicrob. Agents Chemother.* 55 (2011) 947–953.

- [11] L. Daury, F. Orange, J.C. Taveau, A. Verchere, L. Monlezun, C. Gounou, R.K. Marreddy, M. Picard, I. Broutin, K.M. Pos, O. Lambert, Tripartite assembly of RND multidrug efflux pumps, *Nat. Commun.* 7 (2016) 10731.
- [12] A. Davin-Regli, M. Masi, S. Bialek, M. Nicolas-Chanoine, J.M. Pages, Helen I. Zgurskaya, Xian-Zhi Li, Christopher A. Elkins (Eds.), *Antimicrobial Drug Efflux Pumps in Enterobacter and Klebsiella. Efflux-mediated Antimicrobial Resistance in Bacteria*, Chapter 7, Springer International Publishing, 2016, pp. 281–306.
- [13] J. Dreier, P. Ruggerone, Interaction of antibacterial compounds with RND efflux pumps in *Pseudomonas aeruginosa*, *Front. Microbiol.* 6 (2015) 660.
- [14] D. Du, H. Venter, K.M. Pos, B.F. Luisi, The machinery and mechanism of multidrug efflux in gram-negative bacteria, in: E.W. Yu, Q. Zhang, M.H. Brown (Eds.), *Microbial Efflux Pumps: Current Research*, Chap. 3, Caister Academic Press, Ames, IA, 2013, pp. 35–48.
- [15] D. Du, J. Voss, Z. Wang, W. Chiu, B.F. Luisi, The pseudo-atomic structure of an RND-type tripartite multidrug efflux pump, *Biol. Chem.* 396 (2015) 1073–1082.
- [16] D. Du, Z. Wang, N.R. James, J.E. Voss, E. Klimont, T. Ohene-Agyei, H. Venter, W. Chiu, B.F. Luisi, Structure of the AcrAB-TolC multidrug efflux pump, *Nature* 509 (2014) 512–515.
- [17] T. Eicher, L. Brandstatter, K.M. Pos, Structural and functional aspects of the multidrug efflux pump AcrB, *Biol. Chem.* 390 (2009) 693–699.
- [18] T. EICHER, H.J. CHA, M.A. SEEGER, L. BRANDSTATTER, J. El-Delik, J.A. Bohnert, W.V. Kern, F. Verrey, M.G. Grutter, K. Diederichs, K.M. Pos, Transport of drugs by the multidrug transporter AcrB involves an access and a deep binding pocket that are separated by a switch-loop, *Proc. Natl. Acad. Sci. U. S. A.* 109 (2012) 5687–5692.
- [19] A.D. Kinana, A.V. Vargiu, H. Nikaido, Effect of site-directed mutations in multidrug efflux pump AcrB examined by quantitative efflux assays, *Biochem. Biophys. Res. Commun.* 480 (2016) 552–557.
- [20] A.D. Kinana, A.V. Vargiu, T. May, H. Nikaido, Aminoacyl beta-naphthylamides as substrates and modulators of AcrB multidrug efflux pump, *Proc. Natl. Acad. Sci. U. S. A.* 113 (2016) 1405–1410.
- [21] X.Z. Li, P. Plesiat, H. Nikaido, The challenge of efflux-mediated antibiotic resistance in gram-negative bacteria, *Clin. Microbiol. Rev.* 28 (2015) 337–418.
- [22] O. Lomovskaya, K.A. Bostian, Practical applications and feasibility of efflux pump inhibitors in the clinic—a vision for applied use, *Biochem. Pharmacol.* 71 (2006) 910–918.
- [23] O. Lomovskaya, M.S. Warren, A. Lee, J. Galazzo, R. Fronko, M. Lee, J. Blais, D. Cho, S. Chamberland, T. Renau, R. Leger, S. Hecker, W. Watkins, K. Hoshino, H. Ishida, V.J. Lee, Identification and characterization of inhibitors of multidrug resistance efflux pumps in *Pseudomonas aeruginosa*: novel agents for combination therapy, *Antimicrob. Agents Chemother.* 45 (2001) 105–116.
- [24] M. Masi, M. Réfregiers, K.M. Pos, J.M. Pages, Mechanisms of envelope permeability and antibiotic influx and efflux in gram-negative bacteria, *Nat Microbiol* (2017), <http://dx.doi.org/10.1038/nmicrobiol.2017.1>.
- [25] S. Murakami, R. Nakashima, E. Yamashita, T. Matsumoto, A. Yamaguchi, Crystal structures of a multidrug transporter reveal a functionally rotating mechanism, *Nature* 443 (2006) 173–179.
- [26] Y. Matsumoto, K. Hayama, S. Sakakihara, K. Nishino, H. Noji, R. Iino, A. Yamaguchi, Evaluation of multidrug efflux pump inhibitors by a new method using microfluidic channels, *PLoS One* 6 (2011) e18547.
- [27] K. Nagano, H. Nikaido, Kinetic behavior of the major multidrug efflux pump AcrB of *Escherichia coli*, *Proc. Natl. Acad. Sci. U. S. A.* 106 (2009) 5854–5858.
- [28] R. Nakashima, K. Sakurai, S. Yamasaki, K. Nishino, A. Yamaguchi, Structures of the multidrug exporter AcrB reveal a proximal multisite drug-binding pocket, *Nature* 480 (2011) 565–569.
- [29] R. Nakashima, K. Sakurai, S. Yamasaki, K. Hayashi, C. Nagata, K. Hoshino, Y. Onodera, K. Nishino, A. Yamaguchi, Structural basis for the inhibition of bacterial multidrug exporters, *Nature* 500 (2013) 102–106.
- [30] H. Nikaido, J.M. Pages, Broad-specificity efflux pumps and their role in multidrug resistance of gram-negative bacteria, *FEMS Microbiol. Rev.* 36 (2012) 340–363.
- [31] H. Nikaido, Structure and mechanism of RND-type multidrug efflux pumps, *Adv. Enzymol. Relat. Areas Mol. Biol.* 77 (2011) 1–60.
- [32] T. Ohene-Agyei, J.D. Lea, H. Venter, Mutations in MexB that affect the efflux of antibiotics with cytoplasmic targets, *FEMS Microbiol. Lett.* 333 (2012) 20–27.
- [33] T. Ohene-Agyei, R. Mowla, T. Rahman, H. Venter, Phytochemicals increase the antibacterial activity of antibiotics by acting on a drug efflux pump, *Microbiology* 3 (2014) 885–896.
- [34] T.J. Opperman, S.T. Nguyen, Recent advances toward a molecular mechanism of efflux pump inhibition, *Front. Microbiol.* 6 (2015) 421.
- [35] K. Poole, Multidrug efflux pumps and antimicrobial resistance in *Pseudomonas aeruginosa* and related organisms, *J. Mol. Microbiol. Biotechnol.* 3 (2001) 255–264.
- [36] K. Poole, Overcoming multidrug resistance in gram-negative bacteria, *Curr. Opin. Investig. Drugs* 4 (2003) 128–139.
- [37] K. Poole, Efflux pumps as antimicrobial resistance mechanisms, *Ann. Med.* 39 (2007) 162–176.
- [38] K. Poole, *Pseudomonas aeruginosa*: resistance to the max, *Front. Microbiol.* 2 (2011) 00065.
- [39] K.M. Pos, Drug transport mechanism of the AcrB efflux pump, *Biochim. Biophys. Acta* 1794 (2009) 782–793.
- [40] K.M. Pos, A. Schiefner, M.A. Seeger, K. Diederichs, Crystallographic analysis of AcrB, *FEBS Lett.* 564 (2004) 333–339.
- [41] M. Puiu, C. Bala, SPR and SPR imaging: recent trends in developing nanodevices for detection and real-time monitoring of biomolecular events, *Remote Sens.* 16 (2016) e870.
- [42] V.K. Ramaswamy, P. Cacciottio, G. Mallocci, A.V. Vargiu, P. Ruggerone, Computational modelling of efflux pumps and their inhibitors, *Essays Biochem.* 61 (2017) 141–156.
- [43] V.K. Ramaswamy, A.V. Vargiu, G. Mallocci, J. Dreier, P. Ruggerone, Molecular rationale behind the differential substrate specificity of bacterial RND multi-drug transporters, *Sci Rep* 7 (2017) 8075.
- [44] P. Ruggerone, S. Murakami, K.M. Pos, A.V. Vargiu, RND efflux pumps: structural information translated into function and inhibition mechanisms, *Curr. Top. Med. Chem.* 13 (2013) 3079–3100.
- [45] T.H. Schmidt, M. Raunest, N. Fischer, D. Reith, C. Kandt, Computer simulations suggest direct and stable tip to tip interaction between the outer membrane channel TolC and the isolated docking domain of the multidrug RND efflux transporter AcrB, *Biochim. Biophys. Acta* 1858 (2016) 1419–1426.
- [46] E.K. Schneider, F. Reyes-Ortega, T. Velkov, J. Li, Antibiotic-non-antibiotic combinations for combating extremely drug-resistant gram-negative ‘superbugs’, *Essays Biochem.* 61 (2017) 115–125.
- [47] M.A. Seeger, A. Schiefner, T. Eicher, F. Verrey, K. Diederichs, K.M. Pos, Structural asymmetry of AcrB trimer suggests a peristaltic pump mechanism, *Science* 313 (2006) 1295–1298.
- [48] S. Seyedmohammad, D. Born, H. Venter, Expression, purification and functional reconstitution of FeoB, the ferrous iron transporter from *Pseudomonas aeruginosa*, *Protein Expr. Purif.* 101 (2014) 138–145.
- [49] S. Seyedmohammad, N.A. Fuentealba, R.A. Marriotti, T.A. Goetze, J.M. Edwardson, N.P. Barrera, H. Venter, Structural model of FeoB, the iron transporter from *Pseudomonas aeruginosa*, predicts a cysteine lined, GTP-gated pore, *Biosci. Rep.* 36 (2016) e00322.
- [50] H. Sjuts, A.V. Vargiu, S.M. Kwasny, S.T. Nguyen, H.S. Kim, X. Ding, A.R. Ornik, P. Ruggerone, T.L. Bowlin, H. Nikaido, K.M. Pos, T.J. Opperman, Molecular basis for inhibition of AcrB multidrug efflux pump by novel and powerful pyranopyridine derivatives, *Proc. Natl. Acad. Sci. U. S. A.* 113 (2016) 3509–3514.
- [51] L. Song, X. Wu, Development of efflux pump inhibitors in antituberculosis therapy, *Int. J. Antimicrob. Agents* 47 (2016) 421–429.
- [52] G. Spengler, A. Kincses, M. Gajdacs, L. Amaral, New roads leading to old destinations: efflux pumps as targets to reverse multidrug resistance in bacteria, *Molecules* 22 (2017) e468.
- [53] **Tackling drug-resistant infections globally: final report and recommendations. The review on antimicrobial resistance. Chaired by JIM ONEILL MAY 2016.**
- [54] Y. Takatsuka, C. Chen, H. Nikaido, Mechanism of recognition of compounds of diverse structures by the multidrug efflux pump AcrB of *Escherichia coli*, *Proc. Natl. Acad. Sci. U. S. A.* 107 (2010) 6559–6565.
- [55] E.B. Tikhonova, H.I. Zgurskaya, Assessment of multidrug efflux assemblies by surface plasmon resonance. Anne H. Delcour (ed.), *bacterial cell surfaces: methods and protocols*, *Methods Mol. Biol.* 966 (2013) 133–155.
- [56] E.B. Tikhonova, Y. Yamada, H.I. Zgurskaya, Sequential mechanism of assembly of multidrug efflux pump AcrAB-TolC, *Chem. Biol.* 18 (2011) 454–463.
- [57] K.A. Tipton, M. Farokhyar, P.N. Rather, Multiple roles for a novel RND-type efflux system in *Acinetobacter baumannii* AB5075, *Microbiology* 62 (2017) e00418.
- [58] A.V. Vargiu, F. Collu, R. Schulz, K.M. Pos, M. Zacharias, U. Kleinekathöfer, P. Ruggerone, Effect of the F610A mutation on substrate extrusion in the AcrB transporter: explanation and rationale by molecular dynamics simulations, *J. Am. Chem. Soc.* 133 (2011) 10704–10707.
- [59] A.V. Vargiu, H. Nikaido, Multidrug binding properties of the AcrB efflux pump characterized by molecular dynamics simulations, *Proc. Natl. Acad. Sci. U. S. A.* 109 (2012) 20637–20642.
- [60] A.V. Vargiu, P. Ruggerone, T.J. Opperman, S.T. Nguyen, H. Nikaido, Molecular mechanism of MBX2319 inhibition of *Escherichia coli* AcrB multidrug efflux pump and comparison with other inhibitors, *Antimicrob. Agents Chemother.* 58 (2014) 6224–6234.
- [61] S. Velamakanni, T. Janvilisri, S. Shahi, H.W. Van Veen, A functional steroid-binding element in an ATP-binding cassette multidrug transporter, *Mol. Pharmacol.* 73 (2008) 12–17.
- [62] H. Venter, A.E. Ashcroft, J.N. Keen, P.J. Henderson, R.B. Herbert, Molecular dissection of membrane-transport proteins: mass spectrometry and sequence determination of the galactose-H⁺ symport protein, GalP, of *Escherichia coli* and quantitative assay of the incorporation of [ring-2-¹³C] histidine and (15)NH(3), *Biochem. J.* 363 (2002) 243–252.
- [63] H. Venter, M.L. Henningsen, S.L. Begg, Antimicrobial resistance in healthcare, agriculture and the environment: the biochemistry behind the headlines, *Essays Biochem.* 61 (2017) 1–10.
- [64] H. Venter, R. Mowla, T. Ohene-Agyei, S. Ma, RND-type drug efflux pumps from gram-negative bacteria: molecular mechanism and inhibition, *Front. Microbiol.* 6 (2015) 377.
- [65] Y. Wang, R. Mowla, L. Guo, A.D. Ogunniyi, T. Rahman, M.A. De Barros Lopes, S. Ma, H. Venter, Evaluation of a series of 2-naphthamide derivatives as inhibitors of the drug efflux pump AcrB for the reversal of antimicrobial resistance, *Bioorg. Med. Chem. Lett.* 27 (2017) 733–739.
- [66] Y. Wang, H. Venter, S. Ma, Efflux pump inhibitors: a novel approach to combat efflux-mediated drug resistance in bacteria, *Curr. Drug Targets* 17 (2016) 702–719.
- [67] Z. Wang, G. Fan, C.F. Hryc, J.N. Blaza, I.I. Serysheva, M.F. Schmid, W. Chiu, B.F. Luisi, D. Du, An allosteric transport mechanism for the AcrAB-TolC multidrug efflux pump, *elife* 6 (2017) e24905.
- [68] A. Ward, C. Hoyle, S. Palmer, J. O’reilly, J. Griffith, M. Pos, S. Morrison, B. Poolman, M. Gwynne, P. Henderson, Prokaryote multidrug efflux proteins of the major facilitator superfamily: amplified expression, purification and characterisation, *J. Mol. Microbiol. Biotechnol.* 3 (2001) 193–200.
- [69] A. Ward, J. O’reilly, N.G. Rutherford, S.M. Ferguson, C.K. Hoyle, S.L. Palmer, J.L. Clough, H. Venter, H. Xie, G.J. Litherland, G.E. Martin, J.M. Wood, P.E. Roberts, M.A. Groves, W.J. Liang, A. Steel, B.J. Mckeown, P.J. Henderson,

- Expression of prokaryotic membrane transport proteins in *Escherichia coli*, *Biochem. Soc. Trans.* 27 (1999) 893–899.
- [70] A. Welch, C.U. Awah, S. Jing, H.W. Van Veen, H. Venter, Promiscuous partnering and independent activity of MexB, the multidrug transporter protein from *Pseudomonas aeruginosa*, *Biochem. J.* 430 (2010) 355–364.
- [71] WHO, Antimicrobial Resistance: Global Report on Surveillance, (2014), p. 2014 <http://www.who.int/drugresistance/documents/surveillancereport/en/>.
- [72] C. Wilyard, The drug-resistant bacteria that pose the greatest health threats, *Nature* 543 (2017) 15.
- [73] B. Woecking, S. Velamakanni, L. Federici, M.A. Seeger, S. Murakami, H.W. Van Veen, Functional role of transmembrane helix 6 in drug binding and transport by the ABC transporter MsbA, *Biochemistry* 47 (2008) 10904–10914.
- [74] A. Yamaguchi, R. Nakashima, K. Sakurai, Structural basis of RND-type multidrug exporters, *Front. Microbiol.* 6 (2015) 327.
- [75] H. Zheng, J. Taraska, A.J. Merz, T. Gonen, The prototypical H⁺/galactose symporter GalP assembles into functional trimers, *J. Mol. Biol.* 396 (2010) 593–601.